IEEE Access
Multidisciplinary | Rapid Review | Open Access Journal

Received March 8, 2021, accepted March 18, 2021, date of publication March 23, 2021, date of current version April 1, 2021.

Digital Object Identifier 10.1109/ACCESS.2021.3068140

A Novel Fixed-Time Control Algorithm for Trajectory Tracking Control of Uncertain Magnetic Levitation Systems

ANH TUAN VO, THANH NGUYEN TRUONG, AND HEE-JUN KANG
Department of Electrical, Electronic and Computer Engineering, University of Ulsan, Ulsan 44610, South Korea

Corresponding author: Hee-Jun Kang (hjkang@ulsan.ac.kr)

This research was supported by Basic Science Research Program through the National Research Foundation of Korea (NRF) funded by the Ministry of Education (NRF-2019R1D1A3A03103528).

ABSTRACT In this research, a new robust control method is developed, which achieves a fixed-time convergence, robust stabilization, and high accuracy for trajectory tracking control of uncertain magnetic levitation systems. A hybrid controller is a combination of an adaptive fixed-time disturbance observer and a fixed-time control algorithm. First, to estimate precisely the total uncertain component in fixed-time, an adaptive disturbance observer is constructed. Then, a new robust control method is designed from a proposed fixed-time sliding manifold, disturbance observer's information, and a continuous fixed-time reaching law. A global fixed-time stability and convergence time boundary of the control system is obtained by Lyapunov criteria in which the settling time can be arbitrarily set using design parameters regardless of the system's initial state. Finally, the designed control strategy is implemented for a magnetic levitation system and its control performance is compared with other existing finite-time control methods to evaluate outstanding features of the proposed system. Trajectory tracking experiments in MATLAB/SIMULINK environment have been performed to exhibit the effectiveness and practicability of the designed approach.

INDEX TERMS Lyapunov criteria, fixed-time control, terminal sliding mode control, magnetic levitation systems, nonlinear control.

I. INTRODUCTION

The design of advanced controllers for magnetic levitation systems (MLSs) is essential to extend their applications to many real systems in automation, transportation, and other related research fields. MLSs have been used very successfully in many fields. Some notable applications stated in studies [1], [2] can be mentioned as a high-speed maglev train, frictionless bearings, spacecraft, rocket-guiding projects, gyroscopes, microrobotics, contactless melting, wafer distribution systems, the centrifuge of nuclear reactor, vibration isolation systems, and so on. Evidently, MLSs are indeed a potential object for researchers. The general feature in all MLSs applications is the absence of mechanical contact and therefore they are free from abrasion and friction. This increases the working efficiency, reduces maintenance costs, and increases the operating life of the system. MLSs are a technology in which an object is suspended in the air environment without assistance other than the electromagnetic forces. These magnetic fields are applied to reverse or offset the gravitational force or any other counter accelerations. Therefore, the characteristics of MLS are high nonlinearity and unstable under the influence of external noise, sensor noise, and undefined dynamic components. And the mathematical equation description of MLSs is nonlinear differential equations.

Various control methodologies are suggested for MLSs such as adaptive control [3], PID [4], [5], robust control [6], the exact linearization control [7], and Fuzzy H∞ robust control [8]. Most of them rely on the linearization of the mathematical model for the nominal working point. For example, with PID controllers [4], [5], although it has a simple design and is easy to design, the performance is not high due to without considering the mathematical model of the system. With the control methods relied on the linearization of the mathematical model, the linearization of the system's

The associate editor coordinating the review of this manuscript and approving it for publication was Wonhee Kim.

mathematical model may be inadequate in the presence of external disturbances, sensor noise, or unknown dynamic components. As a result, the control performance can be rapidly degraded in working operations with the increasing discrepancy between the trajectory system and the nominal working point. Maintaining a high tracking performance along with an efficient control system over a long work journey is a challenge for researchers. On the other hand, the nonlinear control is marked with the following characteristics: 1) simplicity in the control design; 2) a strong ability to compensate for large change dynamics in uncertain systems; 3) the necessary range of work is large. Consequently, nonlinear control algorithms seem more suitable for MLSs than for model linearization. In addition, MLSs also exist the variation of suspending mass and the changes of resistance and inductance due to the process of electromagnet heating. To improve performance, those changes must also be fully considered.

The majority of the nonlinear controllers for MLSs that existed in the literature have only been verified by computer simulation results [9]–[14]. A few studies have also been applied to real systems with low efficiency. Usually, the desired trajectories in those studies are simple as straight lines. For more complex orbits, such as sinusoidal and rest-to-rest, are rarely considered. Therefore, to track those mentioned trajectories with high performance is also one of the motivations of researchers. The next motivation is that the initial value of the system trajectories in the implemented methods is usually set very small and very close to the desired orbit. The amplitudes of the above orbits are also set to small values. Therefore, the problem of fast convergence has not been investigated with a large initial value. Furthermore, using the above methods especially in SMC only finite-time convergence of the sliding surface is guaranteed, whilst the trajectories of the system asymptotically converge to the origin. Consequently, the system state would never reach the origin point in finite-time. In order to increase tracking accuracy, those controllers need to add more control force input. However, in most cases, it is not practical to be limited in terms of equipment and produce unbounded input values. Or it also causes serious chattering when using sliding mode control-based methods.

Terminal sliding mode control (TSMC) is a popular nonlinear control algorithm derived from sliding mode control (SMC) [15]–[18] thus, it not only inherits the advantages of SMC such as ability rejection to system uncertainties and external noise, low insensitivity, and simple control design but also supplies stable convergence in finite-time and high precision. Thanks to these advantages, TSMC is widely used in control design for nonlinear systems [19]–[23]. However, with the first proposed TSMCs, there appears to be a singularity in calculating the time derivative of the sliding mode surface [24], [25]. To solve the singularity problem or to produce faster convergent stability, theoretical breakthroughs have been introduced such as proposed nonsingular TSMC (NTSMC) in [26]–[28] or proposed fast TSMC (FTSMC) in [29]–[31]. Following this development, nonsingular fast TSMC (NFTSMC) [32]–[38] was developed to inherit the advantages of both NTSMC and FTSMC at the same time. NFTSMC not only evades singularity but also eliminates malfunctions during the approach process of arbitrary initial states to the desired trajectories along with a fast stability convergence in finite-time. Therefore, the control system is continuously running in sliding mode, and immutability is always guaranteed. In addition, the settling time for the convergence of the state variables in approaching the sliding surface can be arbitrarily preset with the controllers such as finite-time or fixed-time NFTSMC [33], [39], [40]. However, very few finite-time or fixed-time NFTSMC for MLSs have been verified for their effectiveness by experimental results [22], [41] until now. The feasibility of the controllers is generally only verified by simulation results on the computer using MATLAB/Simulink [17], [32].

A common characteristic of the conventional SMC, TSMC, or NFTSMC-based control methods is that oscillation occurs in the control input which is commonly known as chattering. Those control algorithms apply discontinuous control action with a sign function to control from an arbitrary initial state to the equilibrium point along a user-defined trajectory and provide outstanding robustness to parameter uncertainty and disturbances. Nevertheless, the control action appears chattering phenomenon because of the discontinuity in the control law that is undesirable in most process applications. Chattering can damage the system, impair control performance, and generate heat that heats the device. From there, the operating life of the device is reduced. Hence, chattering needs to be minimized or eliminated to improve performance. The topic of chattering elimination is still attracting researchers now. There are a number of suggested methods for dealing with chattering, such as continuous sliding-mode control methods [68], [69], neural networks-SMC (NN-SMC) [34], [42]–[46], low pass filters [47], [48], quasi-sliding mode [49], fuzzy-SMC [50], high-order-SMC (HOSMC) [51]. Continuous sliding-mode control methods have lesser chattering than discontinuous sliding-mode control methods. They can reduce chattering behavior but cannot completely eliminate this behavior that analyzed in the paper entitled ''Analysis of Chattering in Continuous Sliding-Mode Controllers'' [70]. NN or Fuzzy can arbitrarily estimate any nonlinear terms of the system. Nevertheless, the use of these approaches has a certain complexity as they add the calculation to the control design. Using low-pass filters can damage the information shape of uncertainties or external disturbances when the filter' parameter is not suitably selected. The finite-time convergence of quasi-sliding mode has not been fully confirmed yet when it is combined with other control methods. With HOSMC, the first uses continuous control signals by calculating the integral of the discontinuous control signal. Based on this computation, a continuous compensation term is then added to the control loop to reduce the influence of total

uncertain terms. Nonetheless, the sliding gain of HOSMC is designated the same as the sliding gain of SMC. Furthermore, convergence stability in fixed-time cannot be guaranteed with a traditional HOSMC. Besides, to reduce the chattering behavior of SMC-based methods without losing the control performance, several observers have been introduced such as extended observer [52], high-gain observer (HGO) [53], sliding mode observer (SMO), fuzzy logic observer (FLO) [54], neural network observer (NNO) [55], etc. Comparison between the above observers, SMO has stronger features, so, it usually offers better accuracy of uncertainty and external disturbances. However, the chattering behaviors still significantly persist with traditional SMO. To reduce SMO's chattering behavior while inheriting its powerful properties, high order sliding mode observer (HOSMO) [56], [57] has been proposed. HOSMO can not only reduce chattering behavior but also provide a finite-time convergence. Unfortunately, the traditional HOSMO has not obtained or guaranteed stability in fixed-time yet. That is a limitation when they are applied to real systems where the initial value of the system trajectories is unknown in advance. Recently, the application of disturbance observer (DO) is also a good potential method which has proven its effectiveness in studies [35], [58]–[60]. In [35], [58]–[60], all of the external disturbances and unknown dynamical uncertain terms are first defined as an extended variable which is the total of unknown uncertain components affecting the system. Then, to exactly achieve this total unknown component, thereby supplying for the control loop, a DO is applied. Thanks to this technique, chattering that appeared in the control input is greatly reduced. Because it is only necessary to use a reasonable gain in the reaching control law to compensate for the effects of DO's approximate error. By using a small design value of the reaching control law only generates suitable chattering in the control signal. Especially, because of DO's simplicity it is suitable for applications in real systems without increasing the system's calculation problem. Moreover, according to the author's knowledge, there has not currently stilled an observer that is combined between HOSMO and DO with fixed-time convergence for MLSs. Therefore, our motivation is to develop a new adaptive DO based on HOSMO with the convergence in fixed-time for MLSs.

In the implemented experimental system, the electromagnetic force keeps the metal sphere floating in the air. Mechanical contact with the sphere is absent in this case. The characteristics of this MLS are high nonlinearity and unstable under the influence of external noise, sensor noise, and undefined dynamic components. Accordingly, the development of an efficient control method to achieve and maintain the expected high control performance in the mentioned work condition is not easy.

Consequently, This article designs a completely new control algorithm and differs from the current control methods for MLSs (such as [17], [22], [61]) that existed in the literature. The designed control method is required to operate a high control performance over a long work journey. The implemented controllers are also required to significantly diminish oscillation behavior in the control inputs while providing a fast fixed-time convergence for system state trajectories. And it is especially important to be applicable to practical applications with a design that is not too complicated. New points and contributions of our robust control method, which achieves a fixed-time convergence, robust stabilization, and high accuracy for trajectory tracking control of uncertain MLSs that highlighted as follows:

1) The first new contribution in this paper compared to existing methods for MLSs is an observer with fixed-time convergence is designed to avoid delay in the information delivery of uncertain components to the control loop. The new DO is developed based on HOSMO and dual layers adaptive rule as in [40], [61].
2) A new robust control method is designed from a proposed fixed-time sliding manifold, disturbance observer's information, and a continuous fixed-time reaching law in which the dual layers adaptive technique is used to reject the requirement of upper bound of the total uncertainties.
3) The settling time of the control system can be calculated in advance by assigning the suitable design parameters regardless of the system's initial state.
4) Fixed-time convergence and the effectiveness of the proposed controller has been fully verified by Lyapunov theory and by experimental results for a real MLS.

The remainder of the paper is organized as follows: Nomenclature, the essential lemmas, definitions, as well as the nonlinear mathematical model of the MLS are presented in Section 2. Section 3 is the synthesis process of the proposed algorithm which is carried out in the following three main steps: Firstly, designs an adaptive disturbance observer. Secondly, proposes a fixed-time sliding mode surface. Finally, designs a new composite control method from a proposed fixed-time sliding manifold, disturbance observer's information, and a continuous fixed-time reaching law. Stability analysis and proofs also are given in Section 3. Validation of the proposed controller's efficiency and superiority compared to a few of the existing methods for MLSs is performed in section 4. Finally, this study is closed with some remarks and conclusions.

II. NOMENCLATURE, PRELIMINARY CONCEPTS, AND MODELING OF MAGNETIC LEVITATION SYSTEMS

A. NOMENCLATURE

The nomenclature used in this paper is stated in Table 1.

B. MODELING OF MAGNETIC LEVITATION SYSTEMS

The MLS considered in this paper is depicted in Fig. 1. The object used for attraction is a metal sphere with a specific mass m which is controlled to move along in an invisible vertical line connecting to the centre point of the electromagnet.

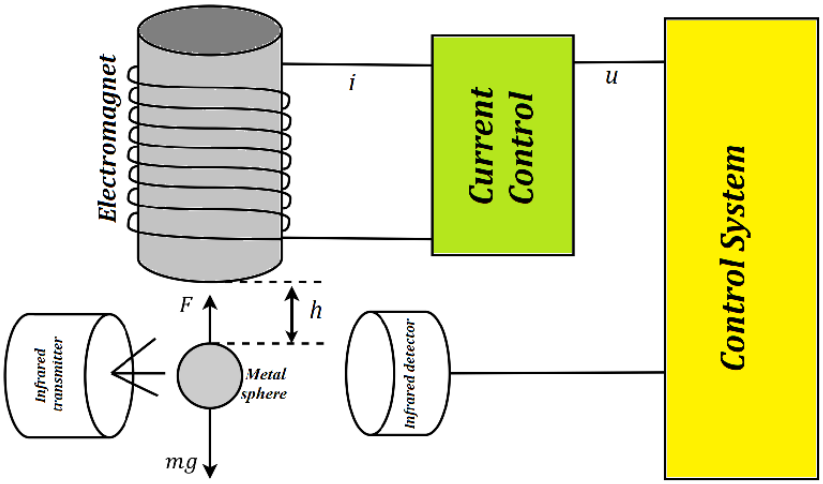

FIGURE 1. Diagram of a Magnetic Levitation System.

TABLE 1. Nomenclature.

Notations	Description
g	gravitational acceleration
h	Position of the metal sphere
h_0	Initial position of the metal sphere
m	Mass of the metal sphere
$\Xi, \hat{\Xi}$	Dynamical parameter of MLS and its estimated value
u	Control voltage input
$u_{\max}$	Maximum control voltage input
i	Current flowing in winding of the electromagnet
$F(h,i)$	Electromagnetic force
β, C	Constant depending on the parameters of the electromagnet and relationship coefficient
$\bar{\delta}, \bar{\delta}^*$	Bounded constant of the total uncertainties and bounded constant of derivative of the total uncertainties
$\mathbb{R}^{n\times m}, \mathbb{R}$	The set of n by m real matrices and real numbers
$\lvert\cdot\rvert$	The absolute value of
$\lVert\cdot\rVert$	The Euclidean norm of
$fal(\cdot)$	function filter
u_{eq}, u_r	Equivalent control and reaching control
$h_d, \dot{h}_d$	The desired position and velocity
$h_{d\min}$	Minimum amplitude of the desired trajectory
$e, \dot{e}$	The positional control error and the velocity control error
s	The sliding surface
$T_{\max}$	Maximum time
T_r	Convergence time in reaching motion phase
T_s	Convergence time in sliding motion phase

The position of the metal sphere is calculated from the underside of the electromagnet to the tip of the metal sphere and it is defined as h. The controller's output signal is a voltage signal u. Then, by using a converter, the output voltage signal will be converted to the current flowing into the coil of the electromagnet. As a result, the electromagnetic force $F(h, i)$ will be generated to reverse and offset the gravitational force or any other counter accelerations as well as to magnetize metal sphere. Therefore, under the effect of the electromagnetic force and gravity, the metal sphere will move in an invisible vertical line connecting to the centre point of the electromagnet. Determining the position of the metal sphere thanks to the use of an infrared sensor to measure the distance between the metal sphere and the electromagnet. This sensor includes infrared transmitters and detectors as displayed in Fig. 1.

The nonlinear model of MLS is presented in a simple formulation based on the studies in [3], [10], [44]:

$$m\ddot{h} = mg - F(h, i), \tag{1}$$

where the acceleration due to the gravity is denoted as g, the electromagnetic force $F(h, i)$ generated by the current flowing in the coil of the electromagnet is determined in the relationship between the current i and the position of the metal sphere h:

$$F(h, i) = \beta\left(\frac{i}{h}\right)^2, \tag{2}$$

where β is a constant depending on the parameters of the electromagnet.

The current flowing in winding and the control input voltage are linearly related according to the expression:

$$i = Cu. \tag{3}$$

where C is a relationship coefficient between the current flowing in winding and the control input voltage.

From the obtained result of Eqs. (2) and (3), Eq. (1) is rewritten as follows:

$$m\ddot{h} = mg - \beta C^2 \frac{1}{h^2}u^2. \tag{4}$$

By dividing both sides of Eq. (4) by m and setting $\Xi = \frac{\beta C^2}{m}$, Eq. (4) can be equivalent:

$$\ddot{h} = g - \frac{\Xi}{h^2}u^2. \tag{5}$$

The system parameter Ξ is not precisely defined, however, this parameter can be achieved by applying approximate methods. In addition, the results shown in Eqs. (2) and (3) can also be obtained by suitable assumptions. Thus, without

a loss of the commonality, Eq. (4) is written in the general form with uncertain dynamics and external disturbances as follows:

$$\ddot{h} = g - \frac{\hat{\Xi}}{h^2}u^2 + \delta(h,t), \tag{6}$$

where $\hat{\Xi}$ is estimate value of Ξ, and $\delta(h,t)$ is a function of uncertain dynamics and external disturbances.

For convenience and to avoid repetition in sentences, the function of uncertain dynamics and external disturbances is termed as the total uncertainties.

Assumption 1: The total uncertainties are assumed to be bounded by:

$$|\delta(h,t)| < \bar{\delta}, \tag{7}$$

where $\bar{\delta}$ is a positive constant.

Assumption 2: The first derivative of the total uncertainties exists:

$$\left|\dot{\delta}(h,t)\right| < \bar{\delta}^*, \tag{8}$$

where $\bar{\delta}^*$ is arbitrary positive constant.

Remark 1: In literature, two assumptions are widely used in the control design [33], [40].

C. MOTIVATION OF THE PAPER

The objective of this research is to propose a new robust control method, which achieves a fixed-time convergence, robust stabilization, and high accuracy for trajectory tracking control of MLSs with uncertain dynamics and external disturbances.

D. PRELIMINARY CONCEPTS

Consider the following system:

$$\dot{x}(t) = f(t,x), \quad x(0) = x_0, \tag{9}$$

where $x \in \mathbb{R}^n$, $f(x)$: δ is nonlinear function that is on open neighborhood $\delta \subseteq \mathbb{R}^n$ of the origin, and $f(0) = 0$. The origin is assumed to be an equilibrium point of the system (9).

Definition 1 ([62]): The origin of the system (9) is called to be a globally finite-time stable if it is globally asymptotically stable with bounded time function $T(x_0)$, i.e., there exists $T_{\max} > 0$ such that $T(x_0)$ satisfies the following constrain $T(x_0) < T_{\max}$.

Lemma 1 ([62]): Let us consider a differential equation:

$$\dot{p} = -k_0 sig(p)^{a_0} - \mu_0 sig(p)^{b_0}, \tag{10}$$

where $sig(p)^{\gamma_i} = |p|^{\gamma_i} sign(p)$, $a_0 = \frac{(\psi_0+1)}{2} + \frac{(\psi_0-1)sign(|p|-1)}{2}$, $b_0 = \frac{(\psi_0+\varphi_0)}{2} + \frac{(\psi_0-\varphi_0)sign(|p|-1)}{2}$, k_0, μ_0 are the designed positive constants, $\psi_0 > 1$, and $0 < \varphi_0 < 1$. Consequently, the dynamic system (10) is admitted as finite-time stable with respect to the initial condition $p(0)$ and the convergence time T_0 is bounded by:

$$T_0 < \frac{1}{(k_0+\mu_0)(\psi_0-1)} + \frac{1}{\mu_0(1-\varphi_0)} \ln\left(1 + \frac{k_0}{\mu_0}\right), \tag{11}$$

III. CONTROL DESIGN AND STABILITY INVESTIGATION

This section presents a new robust control method, which achieves a fixed-time convergence, robust stabilization, and high accuracy for trajectory tracking control of uncertain MLSs.

A. DESIGN OF THE PROPOSED ADAPTIVE DISTURBANCE OBSERVER

The total uncertainties are estimated by the proposed ADO. The proposed observer is designed as:

$$\begin{cases} \tilde{\upsilon} = \upsilon - \dot{h} \\ \dot{\upsilon} = g - \dfrac{\hat{\Xi}}{h^2}u^2 + \hat{\delta} - k_3 sig(\tilde{\upsilon})^{a_3} - \mu_3 sig(\tilde{\upsilon})^{b_3}, \end{cases} \tag{12}$$

where υ represents an estimated value of $\dot{h}$. Furthermore, k_3, μ_3 stand for the positive constants, $a_3 > 1$, and $0 < b_3 < 1$.

The term of $\hat{\delta}$ estimated value of the total uncertainties and its updating law is designed as follows:

$$\begin{cases} \psi = \dot{\tilde{\upsilon}} + k_3 sig(\tilde{\upsilon})^{a_3} + \mu_3 sig(\tilde{\upsilon})^{b_3} \\ \dot{\hat{\delta}} = -k_4 sig(\psi)^{a_4} - \mu_4 sig(\psi)^{b_4} - \bar{\delta}^*(t)\, sign(\psi), \end{cases} \tag{13}$$

where k_4, μ_4 stand for the positive constants, $a_4 > 1$, $0 < b_4 < 1$, and $\bar{\delta}^*(t)$ is an adaptation gain.

Theorem 1: Let us consider the dynamical system (3) if an ADO is designed as Eqs. (12) - (13) to approximate the total uncertainties along with the condition $\bar{\delta}^*(t) > \left|\dot{\delta}\right|$ then ADO's estimation error will converge to zero in fixed-time.

Stability Analysis of ADO:

The first derivative of the term $\tilde{\upsilon}$ in Eq. (12) is calculated as:

$$\begin{aligned} \dot{\tilde{\upsilon}} &= \dot{\upsilon} - \ddot{h} \\ &= \hat{\delta} - \delta - k_3 sig(\tilde{\upsilon})^{a_3} - \mu_3 sig(\tilde{\upsilon})^{b_3}. \end{aligned} \tag{14}$$

Substituting the obtained results in Eq. (14) into Eq. (13), we can gain:

$$\psi = \hat{\delta} - \delta. \tag{15}$$

Taking the time derivative of Eq. (15) and noting Eq. (13), we can attain:

$$\begin{aligned} \dot{\psi} &= \dot{\hat{\delta}} - \dot{\delta} \\ &= -\dot{\delta} - k_4 sig(\psi)^{a_4} - \mu_4 sig(\psi)^{b_4} - \bar{\delta}^*(t)\, sign(\psi). \end{aligned} \tag{16}$$

Define a Lyapunov function candidate $V_1 = 0.5\psi^2$, its time derivative is calculated according to the result in Eq. (16) as follows:

$$\begin{aligned} \dot{V}_1 &= \psi\dot{\psi} \\ &= \psi\left(-\dot{\delta} - k_4 sig(\psi)^{a_4} - \mu_4 sig(\psi)^{b_4} - \bar{\delta}^*(t)\, sign(\psi)\right) \\ &= -\dot{\delta}\psi - \bar{\delta}^*(t)|\psi| - k_4|\psi|^{a_4+1} - \mu_4|\psi|^{b_4+1} \\ &\leqslant -\left(\bar{\delta}^*(t) - \left|\dot{\delta}\right|\right)|\psi| - k_4|\psi|^{a_4+1} - \mu_4|\psi|^{b_4+1} \\ &\leqslant -k_4|\psi|^{a_4+1} - \mu_4|\psi|^{b_4+1} \\ &\leqslant 0. \end{aligned} \tag{17}$$

From Eq. (17), it is easy to see that $\dot{V}_1 \leqslant 0$. Therefore, the sliding mode surface ψ will converge to zero in fixed-time, i.e., $\psi = 0$.

Based Eq. (15), it is seen that ADO's estimation error is defined as:

$$\tilde{\delta} = \hat{\delta} - \delta = \psi. \tag{18}$$

Therefore, ADO can exactly estimate the total uncertainties in fixed-time.

This completes the proof.

The sliding value $\bar{\delta}^*(t)$ was assigned based on Assumption 2. To satisfy this Assumption, $\bar{\delta}^*(t)$ is adapted according to the dual layers adaptive rule as in [40], [63], as follows:

$$\begin{cases} \dot{\bar{\delta}}^*(t) = -(K_0 + K_1)\, sign(\sigma) \\ \dot{K}_1(t) = \begin{cases} K_d\,|\sigma|, & |\sigma| > \sigma_0 \\ 0, & |\sigma| \leqslant \sigma_0 \end{cases} \end{cases} \tag{19}$$

in which

$$\begin{cases} \sigma = \bar{\delta}^*(t) - \dfrac{|\xi|}{\rho_0} - \rho_1 \\ \dot{\xi} = \lambda fal\left(-\bar{\delta}^*(t)\, sign(\psi) - \xi, \eta, \phi_0\right) \\ fal(X, \eta, \phi_0) = \begin{cases} |X|^{\eta} sign(X), & |X| > \phi_0 \\ \dfrac{X}{\phi_0^{1-\eta}}, & |X| \leqslant \phi_0, \end{cases} \end{cases} \tag{20}$$

where $K_0, K_d, \lambda > 0$, $0 < \rho_0, \rho_1, \eta, \phi_0 < 1$. An approximation value of the term $-\bar{\delta}^*(t)\, sign(\psi)$ is achieved by the $fal(\cdot)$ function filter in real-time.

B. DESIGN OF THE PROPOSED FIXED-TIME SLIDING MODE SURFACE

Let h_d be the prescribed reference path. Therefore, $e = h - h_d$ is the positional control error, $\dot{e} = \dot{h} - \dot{h}_d$ is the velocity control error. From tracking errors and Lemma 1, a new fixed-time sliding mode surface is developed to achieve a fast stabilization and fixed-time convergence as follows:

$$s = \dot{e} + k_1 sig(e)^{a_1} + \mu_1 sig(e)^{b_1}, \tag{21}$$

where $s \in \mathbb{R}$ is the fixed-time sliding mode surface, k_1, μ_1 are the designed positive constants, $sig(e)^{\gamma_i} = |e|^{\gamma_i} sign(e)$, $a_1 = \frac{(\psi_1+1)}{2} + \frac{(\psi_1-1) sign(|e|-1)}{2}$, $b_1 = \frac{(\psi_1+\varphi_1)}{2} + \frac{(\psi_1-\varphi_1) sign(|e|-1)}{2}$, $\psi_1 > 1$, and $0 < \varphi_1 < 1$.

According to SMC algorithms, when the system states work in the sliding motion phase, they must be satisfied with some constraints [64]. Therefore, expression (21) becomes:

$$\dot{e} = -k_1 sig(e)^{a_1} - \mu_1 sig(e)^{b_1}. \tag{22}$$

Theorem 2: Let us investigate the dynamics (22) with a globally fixed-time stable point, $e = 0$, and the state variables of the dynamic (22), $e = 0$, within the fixed-time $T_s < \frac{1}{(k_1+\mu_1)(\psi_1-1)} + \frac{1}{\mu_1(1-\varphi_1)} \ln\left(1 + \frac{k_1}{\mu_1}\right)$.

Proof: The differential formula for the dynamics (22) can be equivalent modified as follows:

$$\begin{cases} \dot{e} = -k_1 sig(e)^{\psi_1} - \mu_1 sig(e)^{\psi_1}, & |e| > 1 \\ \dot{e} = -k_1 e - \mu_1 sig(e)^{\varphi_1}, & |e| < 1. \end{cases} \tag{23}$$

where $sig(e)^{\gamma_i} = |e|^{\gamma_i} sign(e)$.

Consequently, the settling time can be obtained by solving Eq. (23):

$$\begin{aligned} T_{\max} &= \lim_{e(0)\to\infty} \left(\int_1^{e(0)} \frac{1}{(k_1+\mu_1)\, sig(e)^{\psi_1}} de \right) \\ &\quad + \lim_{e(0)\to\infty} \left(+ \int_0^1 \frac{1}{k_1 e + \mu_1 sig(e)^{\varphi_1}} de \right) \\ &= \lim_{e(0)\to\infty} \frac{1 - |e(0)|^{1-\psi}}{(k_1+\mu_1)(\psi_1 - 1)} \\ &\quad + \frac{1}{\mu_1(1-\varphi_1)} \ln\left(1 + \frac{k_1}{\mu_1}\right) \\ &= \frac{1}{(k_1+\mu_1)(\psi_1-1)} \\ &\quad + \frac{1}{\mu_1(1-\varphi_1)} \ln\left(1 + \frac{k_1}{\mu_1}\right). \end{aligned} \tag{24}$$

This completes the proof.

C. DESIGN OF THE PROPOSED FIXED-TIME CONTROL ALGORITHM

In this subsection, a new fixed-time control method is devised based on the designed ADO and fixed-time sliding mode surface to achieve high control performance for MLSs (6).

To find the effective control input, the time derivative of Eq. (21) is calculated by:

$$\dot{s} = \ddot{e} + k_1 a_1 |e|^{a_1 - 1} \dot{e} + \mu_1 b_1 |e|^{b_1 - 1} \dot{e}. \tag{25}$$

Then, the dynamic (25) can be rewritten along with the system (6) as:

$$\begin{aligned} \dot{s} = g - \frac{\hat{\Xi}}{h^2} u^2 + \delta - \ddot{h}_d \\ + k_1 \alpha_1 |e|^{a_1 - 1} \dot{e} + \mu_1 b_1 |e|^{b_1 - 1} \dot{e}. \end{aligned} \tag{26}$$

Based on dynamic (26), the control signals are designed as:

$$u = \sqrt{\frac{h^2}{\hat{\Xi}} (u_{eq} + u_r)}, \tag{27}$$

where the term of u_{eq}, holds the path of the error variables on the fixed-time sliding surface (21) and treats the total uncertainties. Therefore, u_{eq} is defined from ADO (12) - (13) and dynamic (26) as follows:

$$u_{eq} = g + \hat{\delta} - \ddot{h}_d + k_1 a_1 |e|^{a_1 - 1} \dot{e} + \mu_1 b_1 |e|^{b_1 - 1} \dot{e}. \tag{28}$$

To handle the remaining influences from the term $\tilde{\delta}$ and to provide a fast convergence for the system trajectory in approaching the proposed sliding mode surface, the reaching control law is suggested in the below expression:

$$u_r = k_2 sig(s)^{a_2} + \mu_2 sig(s)^{b_2}, \tag{29}$$

where k_2, μ_2 are the designed positive constants, $sig(s)^{\gamma_i} = |s|^{\gamma_i} sign(s)$, $a_2 = \frac{(\psi_2+1)}{2} + \frac{(\psi_2-1) sign(|s|-1)}{2}$, $b_2 = \frac{(\psi_2+\varphi_2)}{2} + \frac{(\psi_2-\varphi_2) sign(|s|-1)}{2}$, $\psi_2 > 1$ and $0 < \varphi_2 < 1$.

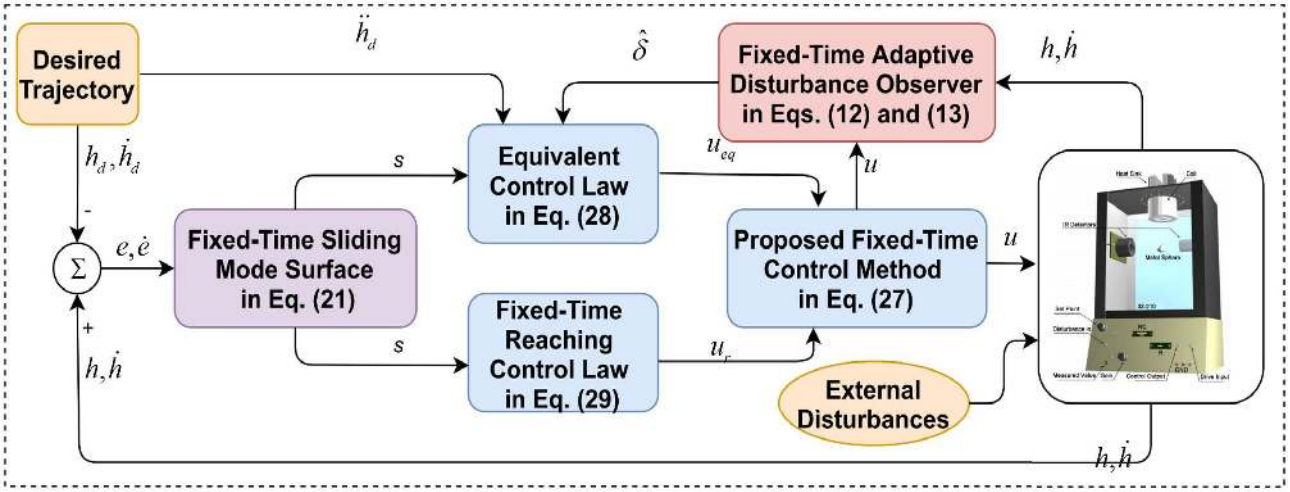

FIGURE 2. The architecture of the proposed fixed-time control methodology.

D. STABILITY INVESTIGATION OF THE DESIGNED CONTROL ALGORITHM

Utilizing the control input signals (27) - (29) to the expression in Eq. (26) offers:

$$\dot{s} = -u_r - \tilde{\delta}. \tag{30}$$

Then, the following Lyapunov candidate $V_2 = s^2$ is considered to verify correctness of the suggested control input (27) - (29) and its time derivative is computed as:

$$\begin{aligned}\dot{V}_2 &= 2s\dot{s} \\ &= 2s\left(-u_r - \tilde{\delta}\right) \\ &= 2s\left(-k_2|s|^{a_2}sign\,(s) - \mu_2|s|^{b_2}sign\,(s) - \tilde{\delta}\right) \\ &= -2k_2|s|^{a_2+1} - 2\mu_2|s|^{b_2+1} - 2\tilde{\delta}s. \end{aligned} \tag{31}$$

As concluded in the subsection of ADO stability analysis, ADO can exactly estimate the total uncertainties in fixed-time. It is means that there exists a fixed-time $\bar{T}$ such that $\tilde{\delta} = 0$ for $t > \bar{T}$, then,

$$\begin{aligned}\dot{V}_2 &= -2k_2|s|^{a_2+1} - 2\mu_2|s|^{b_2+1} \\ &= -2k_2 V_2^{\frac{a_2+1}{2}} - 2\mu_2 V_2^{\frac{b_2+1}{2}}. \end{aligned} \tag{32}$$

Based on Lemma 1, the proposed sliding mode surface will be converged to zero in fixed-time T_r and the convergence time T_r is bounded by

$$T_r < \frac{1}{(k_2+\mu_2)(\psi_2 - 1)} + \frac{1}{\mu_2(1-\varphi_2)} \ln\left(1 + \frac{k_2}{\mu_2}\right). \tag{33}$$

This completes the proof.

Therefore, the total convergence time for the system (6) can be defined as:

$$\begin{aligned}T &= T_r + T_s \\ &< \frac{1}{(k_2+\mu_2)(\psi_2 - 1)} + \frac{1}{\mu_2(1-\varphi_2)} \ln\left(1 + \frac{k_2}{\mu_2}\right) \\ &+ \frac{1}{(k_1+\mu_1)(\psi_1 - 1)} + \frac{1}{\mu_1(1-\varphi_1)} \ln\left(1 + \frac{k_1}{\mu_1}\right). \end{aligned} \tag{34}$$

The architecture of the proposed fixed-time control methodology is depicted in Fig. 2.

TABLE 2. Essential parameters of an experimental MLS.

System parameters	Value	Unit
g	9.81	m/s^2
β	$2.48315625 \times 10^{-5}$	Nm^2/A^2
m	0.02	kg
$\hat{\Pi}$	0.00136884	$(N.m^2)/(kg.V^2)$
C	1.05	A/V

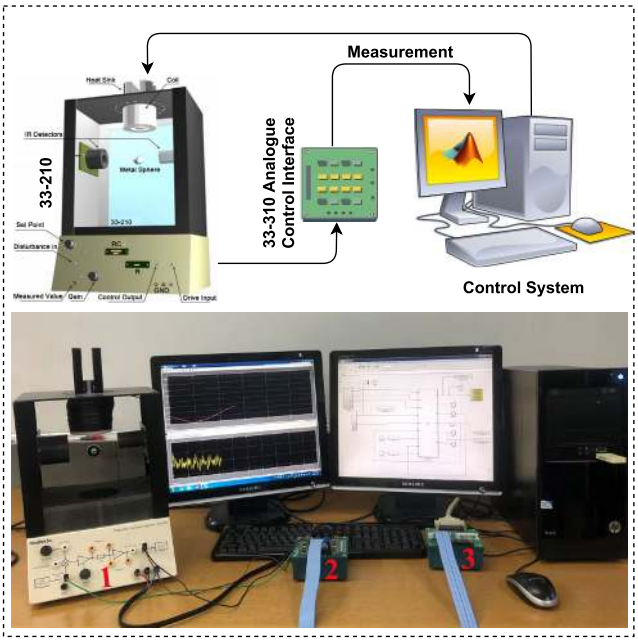

FIGURE 3. Platform of an Experimental MLS.

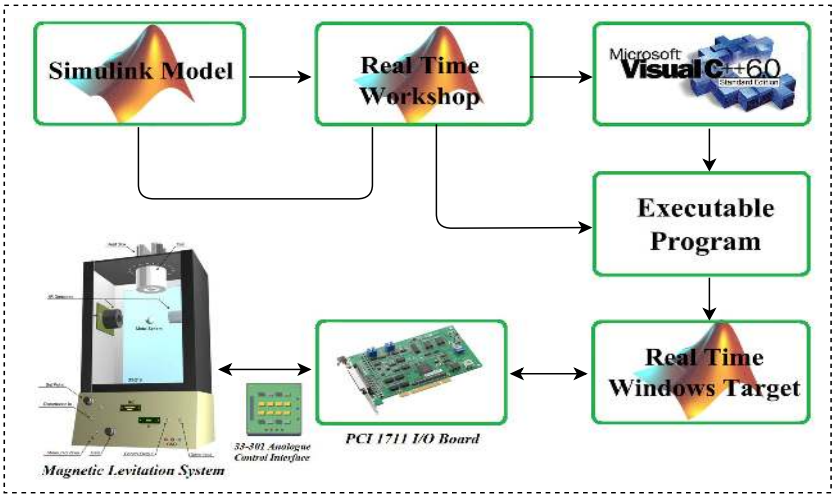

FIGURE 4. Development Tools for the control methodology.

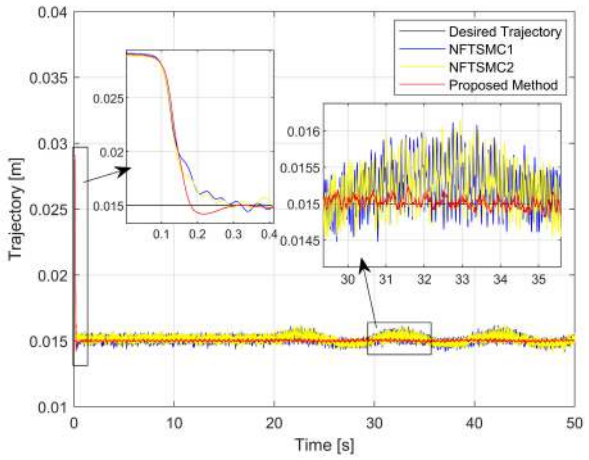

(a) Tracking a straight-line trajectory (36) and the effect of the assumed disturbance (35) in case 1

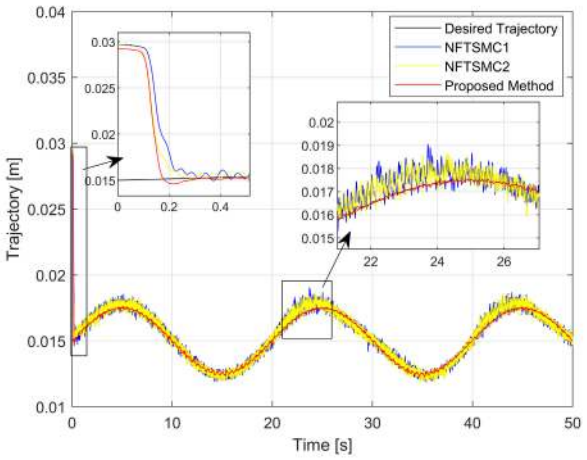

(b) Tracking a sinusoidal trajectory (38) and the effect of the assumed disturbance (37) in case 2

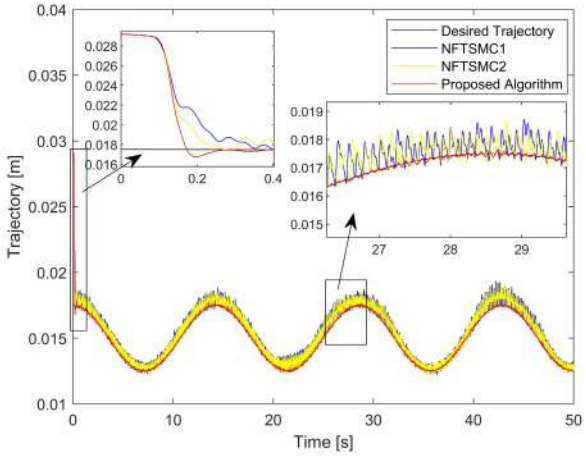

(c) Tracking a sinusoidal trajectory (40) and the effect of the assumed disturbance (39) in case 3

FIGURE 5. The actual trajectories of the metal sphere in tracking the desired trajectories.

IV. EXPERIMENTAL RESULTS AND DISCUSSION

Experimental study of a magnetic levitation system (MLS) has been implemented to investigate the effectiveness of the proposed control algorithm. Trajectory tracking experimental for an experimental MLS [65] has been performed using MATLAB/SIMULINK along with discussions in comparing

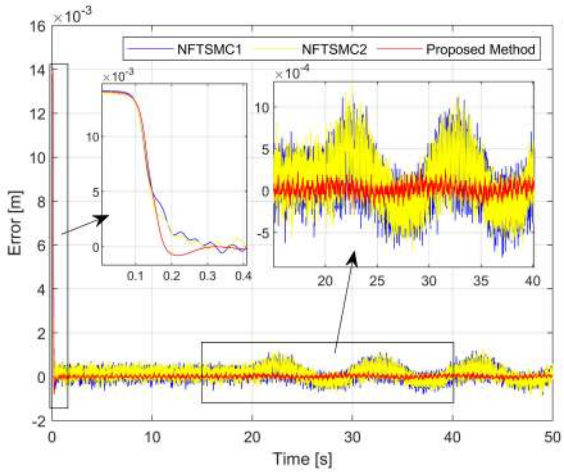

(a) Tracking a straight-line trajectory (36) and the effect of the assumed disturbance (35) in case 1

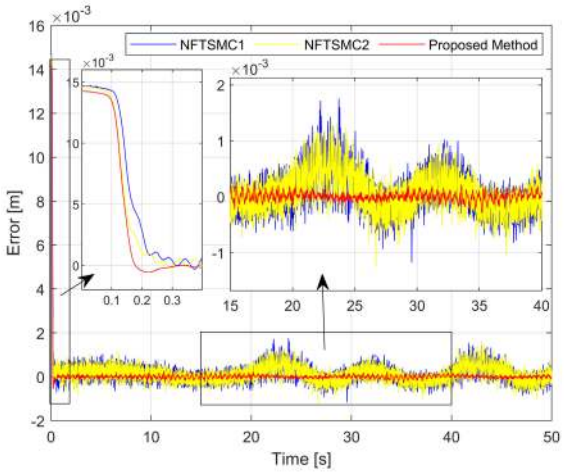

(b) Tracking a sinusoidal trajectory (38) and the effect of the assumed disturbance (37) in case 2

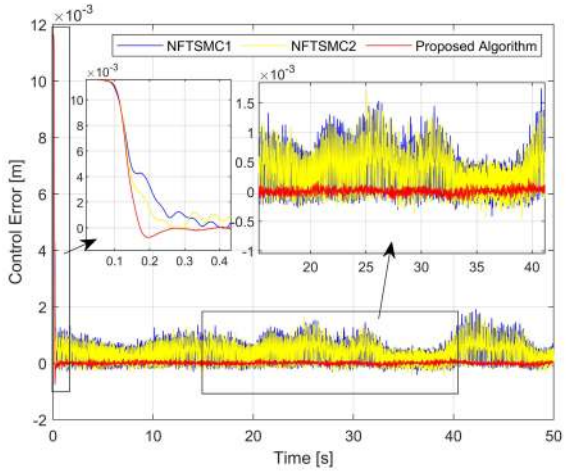

(c) Tracking a sinusoidal trajectory (40) and the effect of the assumed disturbance (39) in case 3

FIGURE 6. **The trajectory errors of the metal sphere in tracking the desired trajectories.**

the performance of the proposed controller with a finite-time NFTSMC stated in [66] and a finite-time NFTSMC stated in [67] to verify the improved performance of the designed control method.

Essential parameters of MLS are reported in Table 2. These parameters were stated in our previous works [34] and an existed study [65].

To validate the performance of the proposed control system by using experimental results, experiments for an MLS were performed under different operating conditions, including the tracking of different desired trajectories as well as the effects of different external disturbances that divides the three following cases:

Case 1: Assume that an external disturbance with the equation described below affects the system:

$$d\left(t\right) = 2\sin\left(\pi t/5\right)\left(m/s^2\right). \tag{35}$$

The metal sphere is driven to trace the straight line as follows:

$$h_{d1} = 15\,(mm)\,, \tag{36}$$

Case 2: Assume that an external disturbance with the equation described below affects the system:

$$d\left(t\right) = 2\sin\left(\pi t/5\right)\left(m/s^2\right). \tag{37}$$

The metal sphere is driven to trace the following sinusoidal line:

$$h_{d2} = 15 + 2.5\sin\left(0.4\pi t\right)(mm)\,. \tag{38}$$

Case 3: Assume that an external disturbance with the equation described below affects the system:

$$d\left(t\right) = 1\sin\left(\pi t/10\right) + 0.8\sin\left(\pi t/5\right) + 0.8\sin\left(2\pi t/5\right)\left(m/s^2\right). \tag{39}$$

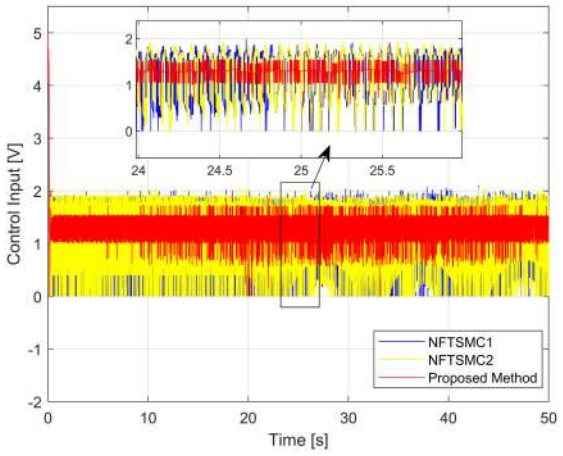

(a) Tracking a straight-line trajectory (36) and the effect of the assumed disturbance (35) in case 1

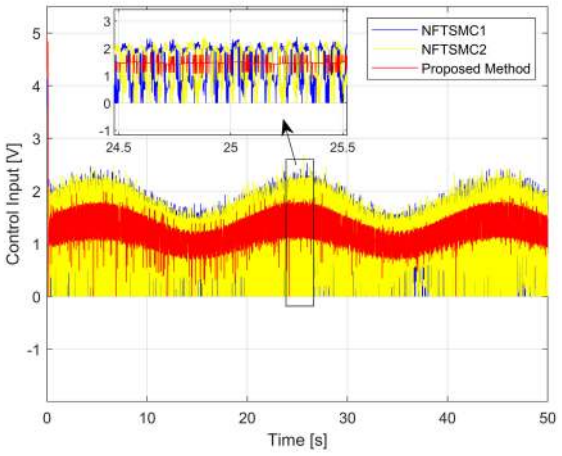

(b) Tracking a sinusoidal trajectory (38) and the effect of the assumed disturbance (37) in case 2

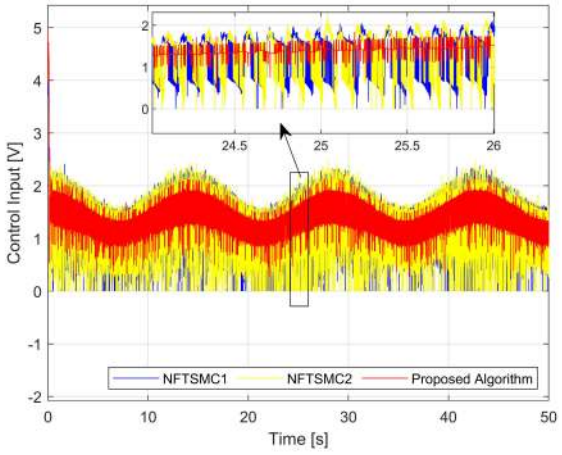

(c) Tracking a sinusoidal trajectory (40) and the effect of the assumed disturbance (39) in case 3

FIGURE 7. **Control input signals of the three separate control methodologies.**

The metal sphere is driven to trace the sinusoidal line as follows:

$$h_{d3} = 15 + 2.5\cos\left(7\pi t/50\right)(mm)\,. \tag{40}$$

Considering Eqs. (38) and (40), they indicate that $h_{d2\min} = h_{d3\min} = 12.5\,(mm)$. The maximum voltage from the output of the controller is limited as $u_{\max} < 4.5\,(V)$. $\Xi = 0.00134557$ is the real value of system dynamic and it is hypothesized according to the experimental results presented in [10]. Based on Assumption 2, the upper bound of the derivative of the total uncertainties is defined:

$$\left|\dot{\delta}\,(h,t)\right| \leqslant \frac{\left|\Xi - \hat{\Xi}\right|}{h_{\min}^2} u_{\max}^2 = 3 \tag{41}$$

in which the system trajectory has initial value of $h_0 = 26\,(mm)$.

To make a comparison of the experimental results from different controllers, a finite-time NFTSMC stated in [66] and a finite-time NFTSMC stated in [67] have been designed for an above MLS as follows:

$$\begin{cases} s = \dot{e} + k_5 sig(e)^{a_5} + \mu_5 sig(e)^{b_5} \\ u = \sqrt{\dfrac{h^2}{\hat{\Xi}}\left(\begin{array}{c} g - \ddot{h}_d + \left(k_5 a_5 |e|^{a_5 - 1} + \mu_5 b_5 |e|^{b_5 - 1}\right)\dot{e} \\ +\Gamma_5 s + \left(\bar{\delta}^* + w_5\right) sign\,(s) \end{array}\right)} \end{cases} \tag{42}$$

and

$$\begin{cases} s = \dot{e} + k_6 sig(e)^{a_6} + \mu_6 sig(e)^{b_6} \\ u = \sqrt{\dfrac{h^2}{\hat{\Xi}}\left(\begin{array}{c} g - \ddot{h}_d + \left(k_6 a_6 |e|^{a_6 - 1} + \mu_6 b_6 |e|^{b_6 - 1}\right)\dot{e} \\ +\Gamma_6 s + \left(\bar{\delta}^* + w_6\right) sign\,(s) \end{array}\right)} \end{cases}. \tag{43}$$

Here, k_5, k_6, μ_5, μ_6 stand for the positive constants, $a_5 > 1$, and $0 < b_5 < 1$. $a_6 = \frac{(\psi_6+1)}{2} + \frac{(\psi_6-1)sign(|e|-1)}{2}$, $b_6 = \frac{(\psi_6+\varphi_6)}{2} + \frac{(\psi_6-\varphi_6)sign(|e|-1)}{2}$, $\psi_6 > 1$, and $0 < \varphi_6 < 1$.

An experimental platform of MLS is setup as our previous work [34] shown in Fig. 3. The experimental system includes

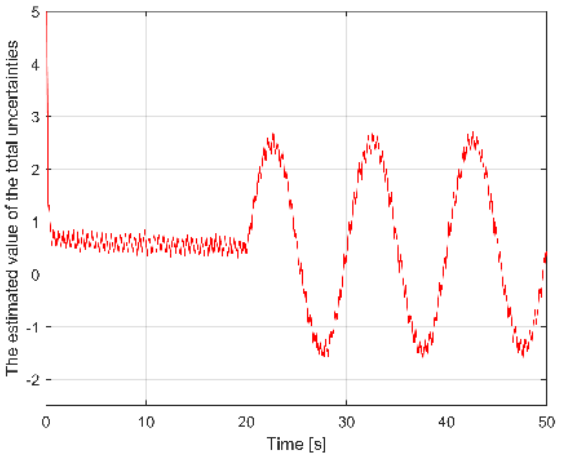

(a) Tracking a straight-line trajectory (36) and the effect of the assumed disturbance (35) in case 1

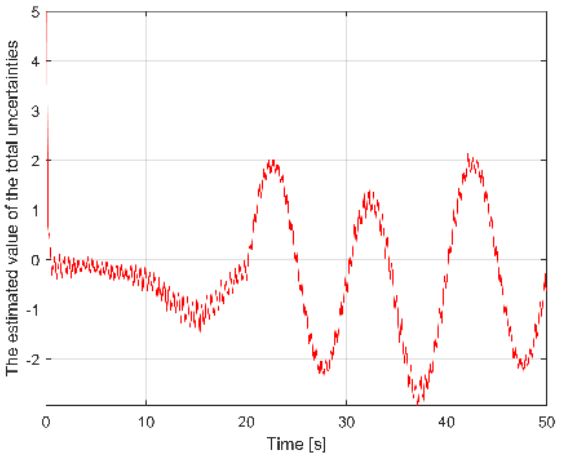

(b) Tracking a sinusoidal trajectory (38) and the effect of the assumed disturbance (37) in case 2

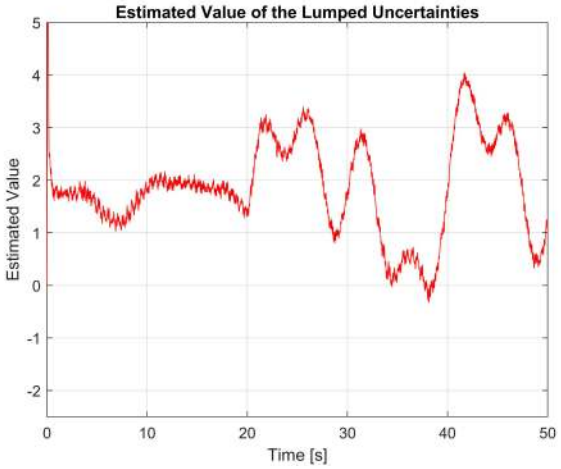

(c) Tracking a sinusoidal trajectory (40) and the effect of the assumed disturbance (39) in case 3

FIGURE 8. Estimated value of the total uncertainties.

number 1) a mechanical component; number 2) analogue control interface; number 3) feedback SCSI adapter box; number 4) a PCI1711 I/O card.

The essential tools for implementation of the control algorithm are displayed in Fig. 4. The fundamental tools include MATLAB/Simulink, Real Time Workshop, Real Microsoft Visual C++ Professional, Control Toolbox, and Time Windows Target. Furthermore, to achieve the executable file from the control law model, the essential processes are performed as in [65].

Remark 2: To facilitate naming control methods in the analysis and evaluation of experiments, the controllers presented in Eqs. (42) and (43) are called NFTSMC1 and NFTSMC2, respectively.

Remark 3: Selection and attainment of control parameters for all three control methods must abide by the following conditions: 1) must comply with the conditions stated in the paper; 2) to ensure the fairness of the comparison among the control methods; 3) the selection of control parameters is carried out by a series of repeated experiments to achieve the best control performance for the three control methods. Consequently, the selection of control parameters for the three control algorithms is reported in Table 3.

Remark 4: First, design parameters k_i and μ_i are selected as positive constant to guarantee the stability of the system. Based on Eq. (11), Eq. (24), or Eq. (34), it is seen that this selection of control parameters affects the control performance. If the coefficients are selected larger, the convergence rate is faster. However, the choice of parameters to satisfy the hardware configuration should also be considered. Therefore, through the practical experiments, we obtain the parameters that are almost optimal for the system.

The performance investigation of the three controllers was conducted in two phases:

Phase 1: At time $0 < t < 20s$, MLS only is checked with uncertain dynamics without the effects of external disturbances that means $d(t) = 0$.

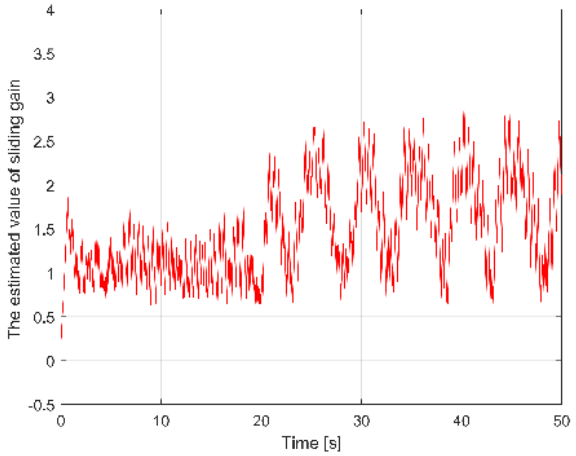

(a) Tracking a straight-line trajectory (36) and the effect of the assumed disturbance (35) in case 1

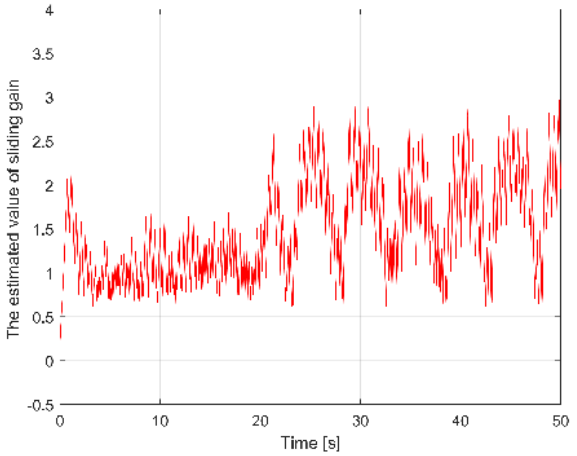

(b) Tracking a sinusoidal trajectory (38) and the effect of the assumed disturbance (37) in case 2

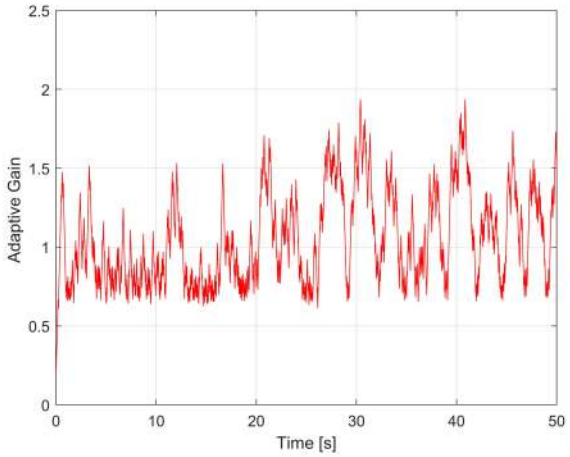

(c) Tracking a sinusoidal trajectory (40) and the effect of the assumed disturbance (39) in case 3

FIGURE 9. Estimated value of the sliding gain.

TABLE 3. The control parameters.

Control System	Symbol	Value
NFTSMC1	k_5, μ_5, a_5	$7, 7, 1.6$
	$b_5, \Gamma_5, \bar{\delta}^* + w$	$0.8, 50, 5$
NFTSMC2	k_6, μ_6, ψ_6	$7, 7, 1.6$
	$\varphi_6, \Gamma_6, \bar{\delta}^* + w$	$0.8, 50, 5$
Designed Method	$k_1, \mu_1, \psi_1, \varphi_1$	$7, 7, 1.6, 0.8$
	$k_2, \mu_2, \psi_2, \varphi_2$	$50, 10, 1.6, 0.8$
ADO	k_3, μ_3, a_3, b_3	$2, 2, 1.7, 0.8$
	k_4, μ_4, a_4, b_4	$3, 3, 1.7, 0.8$
	$K_0, K_d, \sigma_0, \rho_0, \rho_1$	$2, 3, 0.5, 0.6, 0.6$
	λ, η, ϕ_0	$4, 0.7, 0.7$

Phase 2: At time $t = 20s$, an external disturbance is assumed to add to the MLS. Specifically, in three cases, the assumed value of the external disturbance is respectively described in Eqs. (35), (37), and (39).

The position trajectory of the metal sphere in tracking the desired reference trajectory in Eqs. (36), (38), and (40) by using the three other control methodologies is displayed in Fig. 5. The trajectory error of each controller in comparison with the specified trajectory is shown in Fig. 6. An overview in Fig. 5 shows that all three control methods provided high tracking accuracy with fast finite-time convergence. Accordingly, they can be used for the trajectory tracking control of uncertain MLSs. Considering in detail the trajectory error generated by the three control methods, it is seen that NFTSMC1 and NFTSMC2 produce the same trajectory errors. The tracking accuracy of both methods including NFTSMC1 and NFTSMC2 can be achieved which is on the order of $10^{-3} \sim 10^{-4}m$. And their convergence time also can be obtained $T \approx 0.3s$. However, the convergence time of NFTSMC2 is a little faster than the convergence time of NFTSMC1. Meanwhile, the proposed control methodology has the smallest trajectory errors ($10^{-4} \sim 10^{-5}m$) along with the fastest convergence time ($T \approx 0.2s$) among the three control methods.

Fig. 7 shows the control input signals of three different control methods. The chattering behavior is also clearly displayed in Fig. 7. Performing a comparison of chattering

behavior among the three controllers we noticed that the chattering behavior appeared in the control signals of both NFTSMC1 and NFTSMC2 has the same amplitude and frequency. Because NFTSMC1 and NFTSMC2 have applied the same gain value (with $\bar{\delta}^* + w = 5$) in the reaching control law to dismiss the undesired effects of total uncertainties. The chattering behavior that appeared in the control signal of the proposed controller has been significantly reduced because the total uncertainties have been estimated by an ADO to feed to the closed control loop. Moreover, a continuous fixed-time reaching law in Eq. (29) also contributes to reducing chattering behavior. In the theory of continuous SMC, most of continuous sliding-mode controllers can deliver smooth signals with no chattering. However, as we are known, Chattering is fast oscillations caused by finite-time or fixed-time controllers due to the system's non-idealities and it does not matter if it is a continuous controller or not. That is why it is impossible to conclude about finite-time or fixed-time chattering-free control. The continuous SMC only provides the control signal without chattering phenomena in simulation conditions. For the real system, this seems to be impossible. In fact, our experiments it has shown that it only significantly reduces chattering but cannot eliminate completely chattering behavior. In addition, because the characteristic of the system under consideration is the electromagnetic force keeps the metal sphere floating in the air. Mechanical contact with the sphere is absent in this case. Therefore, the characteristic of the control input appears the oscillations as shown in Fig. 7.

Fig. 8 displays the estimated value of the total uncertainties. Look at Fig. 8, it is seen that ADO has a fixed-time convergence. Therefore, the stability of ADO is guaranteed in fixed-time to avoid delay in the information delivery of uncertain components to the control loop.

The estimated values of the adaptive sliding gain are shown in Fig. 9. Fig. 9 indicates that these values are excellently adapted according to variations of the total uncertainties. With the dual layers adaptive technique, the requirement of upper bound of the total uncertainties was rejected. Moreover, the adaptive values have expressed an increase or decrease according to an increase or decrease of the total uncertainties. It is not the same as traditional adaptive techniques that only show an increase in order to reach the upper bound of the total uncertainties.

The proposed controller proved to be the best of the three control methods from the experimental evaluation results in three terms including the tracking accuracy, fast fixed-time convergence, and chattering behavior.

V. SOME REMARKS AND CONCLUSION

In this research, a new robust control method was developed, which achieved a fixed-time convergence, robust stabilization, and high accuracy for trajectory tracking control of uncertain MLSs. The new points and important contributions of the paper can be marked as follows: 1) an ADO with fixed-time convergence was proposed to avoid delay in the information delivery of uncertain components to the control loop; 2) the settling time of the control system could be calculated in advance by assigning the suitable design parameters regardless of the system's initial state; 3) the adaptive values are excellently adapted according to variations of the total uncertainties. Therefore, the requirement of upper bound of the total uncertainties was rejected. Moreover, the adaptive values have expressed an increase or decrease according to an increase or decrease of the total uncertainties. It is not the same as traditional adaptive techniques that only show an increase in order to reach the upper bound of the total uncertainties; 4) the proposed control algorithm proved to be the best of the three control methods from the experimental evaluation results in three terms including high tracking accuracy, fast fixed-time convergence, and less chattering behavior; 5) fixed-time convergence and the effectiveness of the proposed controller has been fully verified by Lyapunov theory and by experimental results for a real MLS.

It is seen that system (6) has the form of a class of second-order nonlinear systems. Therefore, the implemented control algorithm can extend to various nonlinear systems such as robotic manipulators, inverted pendulums, Van der Pol circuit systems, and so on. Moreover, a robust fault-tolerant control method for MLSs should be considered in future work which not only considers faults in the system but also considers faults from sensors.

REFERENCES

[1] H.-W. Lee, K.-C. Kim, and J. Lee, "Review of maglev train technologies," *IEEE Trans. Magn.*, vol. 42, no. 7, pp. 1917–1925, Jul. 2006.
[2] H. Yaghoubi, "The most important maglev applications," *J. Eng.*, vol. 2013, Mar. 2013, Art. no. 537986.
[3] Z. Zhang and X. Li, "Real-time adaptive control of a magnetic levitation system with a large range of load disturbance," *Sensors*, vol. 18, no. 5, p. 1512, May 2018.
[4] Q. Chen, Y. Tan, J. Li, and I. Mareels, "Decentralized PID control design for magnetic levitation systems using extremum seeking," *IEEE Access*, vol. 6, pp. 3059–3067, 2018.
[5] S. K. Swain, D. Sain, S. K. Mishra, and S. Ghosh, "Real time implementation of fractional order PID controllers for a magnetic levitation plant," *AEU-Int. J. Electron. Commun.*, vol. 78, pp. 141–156, Aug. 2017.
[6] C.-H. Kim, "Robust control of magnetic levitation systems considering disturbance force by LSM propulsion systems," *IEEE Trans. Magn.*, vol. 53, no. 11, Nov. 2017, Art. no. 8300805.
[7] A. Ma'arif, A. I. Cahyadi, and O. Wahyunggoro, "CDM based servo state feedback controller with feedback linearization for magnetic levitation ball system," *Int. J. Adv. Sci., Eng. Inf. Technol.*, vol. 8, no. 3, p. 930, Jun. 2018.
[8] Y.-G. Sun, J.-Q. Xu, C. Chen, and G.-B. Lin, "Fuzzy H∞ robust control for magnetic levitation system of maglev vehicles based on TS fuzzy model: Design and experiments," *J. Intell. Fuzzy Syst.*, vol. 36, no. 2, pp. 911–922, 2019.
[9] T. Bächle, S. Hentzelt, and K. Graichen, "Nonlinear model predictive control of a magnetic levitation system," *Control Eng. Pract.*, vol. 21, no. 9, pp. 1250–1258, Sep. 2013.
[10] R. Morales, V. Feliu, and H. Sira-Ramirez, "Nonlinear control for magnetic levitation systems based on fast online algebraic identification of the input gain," *IEEE Trans. Control Syst. Technol.*, vol. 19, no. 4, pp. 757–771, Jul. 2011.
[11] A. El Hajjaji and M. Ouladsine, "Modeling and nonlinear control of magnetic levitation systems," *IEEE Trans. Ind. Electron.*, vol. 48, no. 4, pp. 831–838, Aug. 2001.
[12] C.-L. Kuo, T.-H.-S. Li, and N. R. Guo, "Design of a novel fuzzy sliding-mode control for magnetic ball levitation system," *J. Intell. Robot. Syst.*, vol. 42, no. 3, pp. 295–316, Mar. 2005.

[13] N. F. Al-Muthairi and M. Zribi, "Sliding mode control of a magnetic levitation system," *Math. Problems Eng.*, vol. 2004, Jun. 2004, Art. no. 657503.
[14] Z.-J. Yang, K. Miyazaki, S. Kanae, and K. Wada, "Robust position control of a magnetic levitation system via dynamic surface control technique," *IEEE Trans. Ind. Electron.*, vol. 51, no. 1, pp. 26–34, Feb. 2004.
[15] S. Sathiyavathi, "Design of sliding mode controller for magnetic levitation system," *Comput. Electr. Eng.*, vol. 78, pp. 184–203, Sep. 2019.
[16] S. Ding and S. Li, "Second-order sliding mode controller design subject to mismatched term," *Automatica*, vol. 77, pp. 388–392, Mar. 2017.
[17] H. M. M. Adil, S. Ahmed, and I. Ahmad, "Control of MagLev system using supertwisting and integral backstepping sliding mode algorithm," *IEEE Access*, vol. 8, pp. 51352–51362, 2020.
[18] A. T. Azar and Q. Zhu, *Advances and Applications in Sliding Mode Control Systems*, vol. 576. Cham, Switzerland: Springer, 2015, doi: 10.1007/978-3-319-11173-5.
[19] Q. Zhang, C. Wang, X. Su, and D. Xu, "Observer-based terminal sliding mode control of non-affine nonlinear systems: Finite-time approach," *J. Franklin Inst.*, vol. 355, no. 16, pp. 7985–8004, Nov. 2018.
[20] Z. Ma and G. Sun, "Dual terminal sliding mode control design for rigid robotic manipulator," *J. Franklin Inst.*, vol. 355, no. 18, pp. 9127–9149, Dec. 2018.
[21] C. Mu and H. He, "Dynamic behavior of terminal sliding mode control," *IEEE Trans. Ind. Electron.*, vol. 65, no. 4, pp. 3480–3490, Apr. 2018.
[22] J. Wang, L. Zhao, and L. Yu, "Adaptive terminal sliding mode control for magnetic levitation systems with enhanced disturbance compensation," *IEEE Trans. Ind. Electron.*, vol. 68, no. 1, pp. 756–766, Jan. 2021.
[23] M. Chen, Q.-X. Wu, and R.-X. Cui, "Terminal sliding mode tracking control for a class of SISO uncertain nonlinear systems," *ISA Trans.*, vol. 52, no. 2, pp. 198–206, Mar. 2013.
[24] L. Wang, T. Chai, and L. Zhai, "Neural-network-based terminal sliding-mode control of robotic manipulators including actuator dynamics," *IEEE Trans. Ind. Electron.*, vol. 56, no. 9, pp. 3296–3304, Sep. 2009.
[25] K.-B. Park and J.-J. Lee, "Comments on 'a robust MIMO terminal sliding mode control scheme for rigid robotic manipulators,'" *IEEE Trans. Autom. Control*, vol. 41, no. 5, pp. 761–762, May 1996.
[26] Z. Hou, P. Lu, and Z. Tu, "Nonsingular terminal sliding mode control for a quadrotor UAV with a total rotor failure," *Aerosp. Sci. Technol.*, vol. 98, Mar. 2020, Art. no. 105716.
[27] H. Rabiee, M. Ataei, and M. Ekramian, "Continuous nonsingular terminal sliding mode control based on adaptive sliding mode disturbance observer for uncertain nonlinear systems," *Automatica*, vol. 109, Nov. 2019, Art. no. 108515.
[28] X. Yao, J. H. Park, H. Dong, L. Guo, and X. Lin, "Robust adaptive nonsingular terminal sliding mode control for automatic train operation," *IEEE Trans. Syst., Man, Cybern., Syst.*, vol. 49, no. 12, pp. 2406–2415, Dec. 2019.
[29] A. T. Vo, H.-J. Kang, and T. N. Truong, "A fast terminal sliding mode control strategy for trajectory tracking control of robotic manipulators," in *Intelligent Computing Methodologies* (Lecture Notes in Computer Science), vol. 12465, D. S. Huang and P. Premaratne, Eds. Cham, Switzerland: Springer, 2020.
[30] T. N. Truong, A. T. Vo, and H.-J. Kang, "A backstepping global fast terminal sliding mode control for trajectory tracking control of industrial robotic manipulators," *IEEE Access*, vol. 9, pp. 31921–31931, 2021, doi: 10.1109/ACCESS.2021.3060115.
[31] C. U. Solis, J. B. Clempner, and A. S. Poznyak, "Fast terminal sliding-mode control with an integral filter applied to a Van Der Pol oscillator," *IEEE Trans. Ind. Electron.*, vol. 64, no. 7, pp. 5622–5628, Jul. 2017.
[32] J. Pan, W. Li, and H. Zhang, "Control algorithms of magnetic suspension systems based on the improved double exponential reaching law of sliding mode control," *Int. J. Control, Autom. Syst.*, vol. 16, no. 6, pp. 2878–2887, Dec. 2018.
[33] M. Van and D. Ceglarek, "Robust fault tolerant control of robot manipulators with global fixed-time convergence," *J. Franklin Inst.*, vol. 358, no. 1, pp. 699–722, Jan. 2021.
[34] T. N. Truong, A. T. Vo, and H.-J. Kang, "Implementation of an adaptive neural terminal sliding mode for tracking control of magnetic levitation systems," *IEEE Access*, vol. 8, pp. 206931–206941, 2020.
[35] A. T. Vo and H.-J. Kang, "A novel fault-tolerant control method for robot manipulators based on non-singular fast terminal sliding mode control and disturbance observer," *IEEE Access*, vol. 8, pp. 109388–109400, 2020.
[36] A. T. Vo and H.-J. Kang, "An adaptive terminal sliding mode control for robot manipulators with non-singular terminal sliding surface variables," *IEEE Access*, vol. 7, pp. 8701–8712, 2019, doi: 10.1109/ACCESS.2018.2886222.
[37] V. A. Tuan and H. Kang, "A new finite time control solution for robotic manipulators based on nonsingular fast terminal sliding variables and the adaptive super-twisting scheme," *ASME J. Comput. Nonlinear Dyn.*, vol. 14, no. 3, Mar. 2019, Art. no. 031002, doi: 10.1115/1.4042293.
[38] M. Boukattaya, N. Mezghani, and T. Damak, "Adaptive nonsingular fast terminal sliding-mode control for the tracking problem of uncertain dynamical systems," *ISA Trans.*, vol. 77, pp. 1–19, Jun. 2018.
[39] M. L. Corradini and A. Cristofaro, "Nonsingular terminal sliding-mode control of nonlinear planar systems with global fixed-time stability guarantees," *Automatica*, vol. 95, pp. 561–565, Sep. 2018.
[40] H. Pan, G. Zhang, H. Ouyang, and L. Mei, "Novel fixed-time nonsingular fast terminal sliding mode control for second-order uncertain systems based on adaptive disturbance observer," *IEEE Access*, vol. 8, pp. 126615–126627, 2020.
[41] M. P. Aghababa and H. P. Aghababa, "A general nonlinear adaptive control scheme for finite-time synchronization of chaotic systems with uncertain parameters and nonlinear inputs," *Nonlinear Dyn.*, vol. 69, no. 4, pp. 1903–1914, Sep. 2012.
[42] J. Fei and C. Lu, "Adaptive sliding mode control of dynamic systems using double loop recurrent neural network structure," *IEEE Trans. Neural Netw. Learn. Syst.*, vol. 29, no. 4, pp. 1275–1286, Apr. 2018.
[43] Y. Yin, H. Niu, and X. Liu, "Adaptive neural network sliding mode control for quad tilt rotor aircraft," *Complexity*, vol. 2017, Oct. 2017, Art. no. 7104708.
[44] Q. V. Doan, T. D. Le, and A. T. Vo, "Synchronization full-order terminal sliding mode control for an uncertain 3-DOF planar parallel robotic manipulator," *Appl. Sci.*, vol. 9, no. 9, p. 1756, 2019.
[45] A. T. Vo and H.-J. Kang, "Adaptive neural integral full-order terminal sliding mode control for an uncertain nonlinear system," *IEEE Access*, vol. 7, pp. 42238–42246, 2019, doi: 10.1109/ACCESS.2019.2907565.
[46] A. T. Vo and H.-J. Kang, "An adaptive neural non-singular fast-terminal sliding-mode control for industrial robotic manipulators," *Appl. Sci.*, vol. 8, no. 12, p. 2562, Dec. 2018.
[47] D. Zhao, C. Li, and Q. Zhu, "Low-pass-filter-based position synchronization sliding mode control for multiple robotic manipulator systems," *Proc. Inst. Mech. Eng., I, J. Syst. Control Eng.*, vol. 225, no. 8, pp. 1136–1148, Dec. 2011.
[48] M.-L. Tseng and M.-S. Chen, "Chattering reduction of sliding mode control by low-pass filtering the control signal," *Asian J. Control*, vol. 12, no. 3, pp. 392–398, Feb. 2010.
[49] K. Adamiak, "Reference sliding variable based chattering-free quasi-sliding mode control," *IEEE Access*, vol. 8, pp. 133086–133094, 2020.
[50] H. Li, J. Wang, H.-K. Lam, Q. Zhou, and H. Du, "Adaptive sliding mode control for interval type-2 fuzzy systems," *IEEE Trans. Syst., Man, Cybern. Syst.*, vol. 46, no. 12, pp. 1654–1663, Dec. 2016.
[51] V. Utkin, "Discussion aspects of high-order sliding mode control," *IEEE Trans. Autom. Control*, vol. 61, no. 3, pp. 829–833, Mar. 2016.
[52] J. Liu, S. Vazquez, L. Wu, A. Marquez, H. Gao, and L. G. Franquelo, "Extended state observer-based sliding-mode control for three-phase power converters," *IEEE Trans. Ind. Electron.*, vol. 64, no. 1, pp. 22–31, Jan. 2017.
[53] A. Alessandri and A. Rossi, "Increasing-gain observers for nonlinear systems: Stability and design," *Automatica*, vol. 57, pp. 180–188, Jul. 2015.
[54] J. Qiu, K. Sun, T. Wang, and H. Gao, "Observer-based fuzzy adaptive event-triggered control for pure-feedback nonlinear systems with prescribed performance," *IEEE Trans. Fuzzy Syst.*, vol. 27, no. 11, pp. 2152–2162, Nov. 2019.
[55] B. Chen, H. Zhang, and C. Lin, "Observer-based adaptive neural network control for nonlinear systems in nonstrict-feedback form," *IEEE Trans. Neural Netw. Learn. Syst.*, vol. 27, no. 1, pp. 89–98, Jan. 2016.
[56] V.-C. Nguyen, A.-T. Vo, and H.-J. Kang, "A non-singular fast terminal sliding mode control based on third-order sliding mode observer for a class of second-order uncertain nonlinear systems and its application to robot manipulators," *IEEE Access*, vol. 8, pp. 78109–78120, 2020, doi: 10.1109/ACCESS.2020.2989613.
[57] V.-C. Nguyen, A.-T. Vo, and H.-J. Kang, "A finite-time fault-tolerant control using non-singular fast terminal sliding mode control and third-order sliding mode observer for robotic manipulators," *IEEE Access*, vol. 9, pp. 31225–31235, 2021, doi: 10.1109/ACCESS.2021.3059897.
[58] D. Ginoya, C. M. Gutte, P. Shendge, and S. Phadke, "State-and-disturbance-observer-based sliding mode control of magnetic levitation systems," *Trans. Inst. Meas. Control*, vol. 38, no. 6, pp. 751–763, Jun. 2016.

[59] T. N. Truong, H.-J. Kang, and A. T. Vo, "An active disturbance rejection control method for robot manipulators," *Intelligent Computing Methodologies* (Lecture Notes in Computer Science), vol. 12465, D. S. Huang and P. Premaratne, Eds. Cham, Switzerland: Springer, 2020.
[60] A. T. Vo, T. N. Truong, and H.-J. Kang, "A novel tracking control algorithm with finite-time disturbance observer for a class of second-order nonlinear systems and its applications," *IEEE Access*, vol. 9, pp. 31373–31389, 2021, doi: 10.1109/ACCESS.2021.3060381.
[61] X.-T. Tran and H.-J. Kang, "A novel adaptive finite-time control method for a class of uncertain nonlinear systems," *Int. J. Precis. Eng. Manuf.*, vol. 16, no. 13, pp. 2647–2654, 2015.
[62] H. Li and Y. Cai, "On SFTSM control with fixed-time convergence," *IET Control Theory Appl.*, vol. 11, no. 6, pp. 766–773, Apr. 2017.
[63] C. Edwards and Y. Shtessel, "Adaptive dual-layer super-twisting control and observation," *Int. J. Control*, vol. 89, no. 9, pp. 1759–1766, Sep. 2016.
[64] N. Derbel, J. Ghommam, and Q. Zhu, *Applications of Sliding Mode Control*, vol. 79. Singapore: Springer, 2017, doi: 10.1007/978-981-10-2374-3.
[65] M. B. Naumovic and B. R. Veselic, "Magnetic levitation system in control engineering education," *FACTA Univ. Ser. Autom. Control Robot.*, vol. 7, no. 1, pp. 151–160, 2008.
[66] L. Yang and J. Yang, "Nonsingular fast terminal sliding-mode control for nonlinear dynamical systems," *Int. J. Robust Nonlinear Control*, vol. 18, pp. 557–569, Oct. 2010.
[67] Y. Tian, Y. Cai, and Y. Deng, "A fast nonsingular terminal sliding mode control method for nonlinear systems with fixed-time stability guarantees," *IEEE Access*, vol. 8, pp. 60444–60454, 2020.
[68] S. Kamal, J. A. Moreno, A. Chalanga, B. Bandyopadhyay, and L. M. Fridman, "Continuous terminal sliding-mode controller," *Automatica*, vol. 69, pp. 308–314, Jul. 2016.
[69] Q. Xu, "Continuous integral terminal third-order sliding mode motion control for piezoelectric nanopositioning system," *IEEE/ASME Trans. Mechatronics*, vol. 22, no. 4, pp. 1828–1838, Aug. 2017.
[70] I. Boiko and L. Fridman, "Analysis of chattering in continuous sliding-mode controllers," *IEEE Trans. Autom. Control*, vol. 50, no. 9, pp. 1442–1446, Sep. 2005.

ANH TUAN VO received the B.S. degree in electrical engineering from the Danang University of Technology, Danang, Vietnam, in 2008, the M.S. degree in automation from the University of Danang–Danang University of Science and Technology, Danang, in 2013, and the Ph.D. degree in electrical engineering from the Graduate School of the University of Ulsan, Ulsan, South Korea, in 2021. He is currently a Postdoctoral Fellow designated from Brain Korea (BK21). He has published more than 20 articles in journals and international conferences. His research interests include intelligent control, sliding mode control and its application, and fault-tolerant control.

THANH NGUYEN TRUONG received the B.S. degree in electrical engineering from the University of Science and Technology, Danang, Vietnam, in 2018. He is currently pursuing the Ph.D. degree with the University of Ulsan, Ulsan, South Korea. His major research interests include robotic manipulators, sliding mode control and its application, and advanced control theory for mechatronics.

HEE-JUN KANG received the B.S. degree in mechanical engineering from Seoul National University, South Korea, in 1985, and the M.S. and Ph.D. degrees in mechanical engineering from The University of Texas at Austin, USA, in 1988 and 1991, respectively. Since 1992, he has been a Professor of electrical engineering with the University of Ulsan. His current research interests include sensor-based robotic application, robot calibration, haptics, robot fault diagnosis, and mechanism analysis.